

BBA 76886

SODIUM+POTASSIUM-ACTIVATED ATPase OF MAMMALIAN BRAIN REGULATION OF PHOSPHATASE ACTIVITY

ALAN C. SWANN and R. WAYNE ALBERS

Laboratory of Neurochemistry, National Institute of Neurological Diseases and Stroke, National Institutes of Health, Bethesda, Md. 20014 (U.S.A.)

(Received August 20th, 1974)

SUMMARY

1. The K^+ -nitrophenylphosphatase activity associated with mammalian brain $(Na^+ + K^+)$ -ATPase displays K^+ activation curves that have intermediary plateaus and maxima in the presence of less than saturating concentrations of Na^+ . Zero Na^+ and saturating Na^+ produce sigmoid K^+ -activation curves with low and high K^+ affinities respectively.

2. ATP inhibits K^+ -activated nitrophenylphosphatase through both competitive and non-competitive mechanisms. ATP is synergistic with Na^+ in the mechanism which converts the enzyme from low to high K^+ affinity.

3. The Na^+ and K^+ interactions can be accounted for by equations which describe a model with separate regulatory sites for Na^+ and K^+ and with a K^+ -requiring catalytic site which is only accessible in one of the two principal conformational states of the enzyme.

4. The effects of ATP can be accounted for by the same model through interactions at a single nucleotide binding site. Inhibition which is competitive with K^+ and non-competitive with substrate arises from stabilization of the inactive enzyme conformation. Inhibition which is non-competitive with K^+ and competitive with substrate results from interactions with the active enzyme conformation. The synergism between Na^+ and ATP appears to arise as a consequence of the formation of phosphoryl enzyme.

5. A model for $(Na^+ + K^+)$ -ATPase is discussed which involves in-phase coupling of subunit interactions as suggested by these studies.

INTRODUCTION

Many properties of $(Na^+ + K^+)$ -ATPase can be related to the properties of ATP-dependent Na^+ and K^+ transport in a manner which produces some insight into the molecular mechanism [1, 2]. The ATPase is considered to be integral to the active transport unit, which spans the plasmalemma. The specificities of transport

Abbreviations: Me_2SO , dimethylsulfoxide; RMS, root mean square error.

and of the ATPase for univalent cations arise from the properties of binding sites on the enzyme which function as ionophores and as ATPase regulators. Vectorial forces for cation transport are generated by a sequence of conformational transitions which are induced by ATP binding to the enzyme, Na^+ -dependent enzyme phosphorylation and K^+ -dependent enzyme dephosphorylation.

More explicit formulations of this concept have included some assumptions about the number and nature of univalent cation sites. Univalent cation activation kinetics are sigmoid indicating multiple binding sites for both Na^+ and K^+ . Na^+ inhibits K^+ activation and the converse also occurs [3]. These observations have been attributed to interactions with a single type of ionophoric sites, which modulate their cation selectivities and affinities as they change their orientation, inward or outward, in the sequential conformational transitions which constitute active transport [1].

Some theoretical advantages arise from a more complex mechanism which couples the outward Na^+ -transport phase of one pump unit with inward K^+ transport or return of free carriers in another unit. Increased efficiency of energy transduction by coupling "spontaneous" conformational changes in some units to "energy-requiring" transitions in others have been discussed [4-7].

Coupling of two or more units which are in the same conformation (in phase) would also have advantages since ATP interacting at one such unit could drive other coupled units to provide the $\text{Na} : \text{K} : \text{ATP}$ stoichiometry of 3 : 2 : 1 reported for erythrocytes [8, 9] or the variable ratios of Na^+ and K^+ transport fluxes observed in squid giant axons [10].

Our previous studies have shown that in the presence of less than saturating concentrations of sodium, K^+ activation of *Electrophorus electrophorus* nitrophenylphosphatase yields complex curves with intermediary plateaus [11]. A heterotropic relaxation model consistent with the theoretical analysis of Tiepel and Koshland [12] has yielded equations which produce good computer simulation of these experimental results [11, 13]. This model postulates an oligomeric enzyme with distinct sets of sodium regulatory sites, potassium regulatory sites, and potassium-activated catalytic sites [11, 13]. Each cation is a competitive inhibitor for the other. Inactive enzyme, in the absence of ligands, is in the tight ("T") form, with the catalytic sites inaccessible; binding of sodium or potassium in appropriate concentrations results in a conformational change to the relaxed ("R") form, which catalytic sites accessible (see Discussion, Fig. 12). This is one of several possible models which describe a system of two interconvertible forms, with differing K values and similar V values.

Electrophorus and mammalian nitrophenylphosphatase kinetics differ in their interactions with nucleotides. ATP acts synergistically with Na^+ in the stimulation of mammalian nitrophenylphosphatase [15]. This effect, while specific for sodium, was reportedly less specific for nucleotide, though the concentration of ATP required was less than that for other effective nucleotides. *Electrophorus* enzyme displays little Na^+ -ATP synergism [16]. Thus, it was important to determine whether one model could, in fact, encompass the wide variations in kinetic behaviour which we observed.

These experiments were designed to test the generality of this model for Na^+ and K^+ effects on the nitrophenylphosphatase reaction catalysed by $(\text{Na}^+ + \text{K}^+)\text{-ATPase}$, and to examine the modulation of nitrophenylphosphatase activity by ATP. We attempt to account for all of these effects in terms of the ability of ATP to stabilize the "T" conformations which is inactive as a nitrophenylphosphatase, but which, in

the presence of ATP and Na^+ , can phosphorylate itself. Phosphorylation is postulated to make the "T enzyme" unstable with respect to the "R enzyme", which is an active phosphatase. However, it will be argued that only the "dephospho-R-enzyme" can hydrolyse nitrophenylphosphatase. These data suggest that both ATP binding and ATP-dependent phosphorylation determine conformational transitions of active transport units and that the transitions of two or more units are coupled in phase.

MATERIALS AND METHODS

Preparation of enzyme

Guinea pigs were obtained from N.I.H. stock and killed by decapitation. Fresh beef brains were obtained from Frederick County Products. NaI-treated deoxycholate microsomes were prepared as described by Nakao et al. [17], except that treatment with 2 M NaI took place in 0.05 M imidazole buffer, pH 7.1.

Materials

β,γ -Methylene ATP and α,β -methylene ADP were obtained from PL Biochemicals. Tris_2ATP and pyruvate kinase were obtained from Sigma Chemical Co.

Assays of nitrophenylphosphatase [16]

Approximately 7 μg of microsomal protein was incubated with 50 mM Tris \cdot HCl, pH 9, 10 mM MgCl_2 , 5 mM dithiothreitol, 10 mM Tris_2 nitrophenylphosphate, and varying concentrations of K^+ , Na^+ , and Tris_2ATP in a total volume of 50 μl . After 15 min incubation the reactions were stopped with 400 μl of 1 M NaOH and *p*-nitrophenol determined at 420 nm. In all cases, activity without K^+ was determined and subtracted from total enzyme activity to yield K^+ -dependent nitrophenylphosphatase. Activity is expressed in arbitrary units. For guinea pig brain, 1 unit is 0.077 $\mu\text{mol} \cdot \text{mg}^{-1} \cdot \text{min}^{-1}$; for beef brain, 1 unit is 0.089 $\mu\text{mol} \cdot \text{mg}^{-1} \cdot \text{min}^{-1}$. In guinea pig, this represents activity in 10 mM K^+ without Na^+ ; in beef, 1 unit is the calculated V for K^+ activation without Na^+ .

Thus, activity of 1 unit represents hydrolysis of about 10^{-8} mol of nitrophenylphosphate in 15 min, a consumption of 2 % of the $5 \cdot 10^{-7}$ mol present in the original reaction mixture. This results in a final inorganic phosphate concentration of 0.2 mM, which is insufficient for any significant effect on nitrophenylphosphatase activity ($K_i \approx 10$ mM). The course of the nitrophenylphosphatase reaction remains linear for 20 min. For experiments involving Na^+ and ATP, an ATP-regenerating system was used, consisting of 4 mM phosphoenolpyruvate and 1 μl /sample pyruvate kinase (rabbit muscle, suspended in 2.2 M $(\text{NH}_4)_2\text{SO}_4$, specific activity 320 $\mu\text{mol}/\text{mg}$ per min). Pyruvate kinase was dialysed against 0.05 M Tris \cdot HCl, pH 9, at 4 °C for 48 h prior to use, to remove ammonium salts.

Computer simulations

We used an iterative least-squares routine for curve fittings. This routine is designated MLAB and has been described previously [11, 18]. Root means squared error values (RMS), which represent the variance of the theoretical curve from the data, are provided by this routine and are given on the graphs where appropriate. Each parameter that is fit also has a "dependency" value, which is an indication of the dependence of the parameter value on the values of other parameters. Ideally,

parameters would be independent of one another, yielding dependency of one; if parameters are almost totally dependent, dependency will be as high as 1 000 000, implying that an essentially infinite assortment of parameter values would provide an equally good fit. Thus, a good simulation requires both low root means squared error and low dependency values. These criteria were met by all simulations reported.

RESULTS

Na⁺ activation of nitrophenylphosphatase

Na⁺ activation of guinea pig brain nitrophenylphosphatase in 1 mM KCl is shown in Fig. 1a. The addition of ATP leads to a striking increase in Na⁺ activation. Fig. 1b shows that, in the presence of dimethylsulfoxide (Me₂SO), Na⁺ activation is much greater, as has previously been reported for other species [16, 19, 20]. However, the activating effect of ATP is greatly diminished in the presence of Me₂SO.

Intermediary plateaus in K⁺ activation of nitrophenylphosphatase

Fig. 2b shows K⁺ activation of nitrophenylphosphatase in the presence of ATP and 3 concentrations of Na⁺. A curve which exhibits an intermediary plateau is

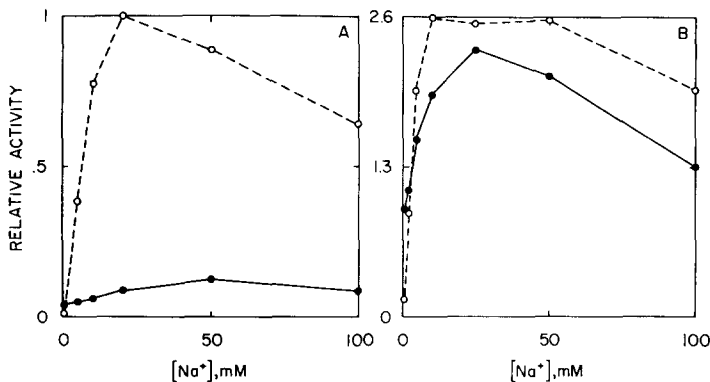


Fig. 1. Na⁺ activation of guinea pig brain K⁺-nitrophenylphosphatase. (A) Aqueous; ●—●, no ATP; ○---○, 0.1 mM ATP. (B) 20% Me₂SO: ●—●, no ATP; ○---○, 0.1 mM ATP.

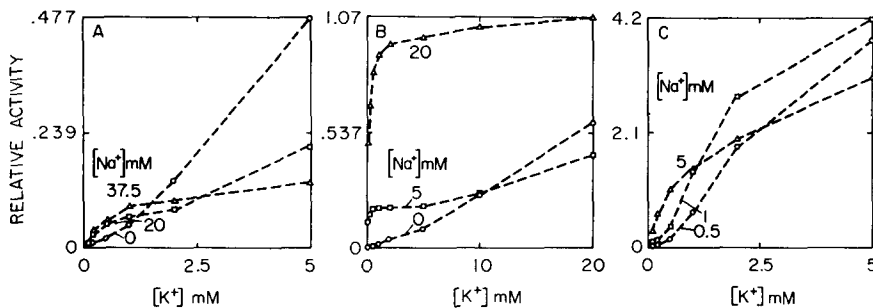


Fig. 2. K⁺ activation of guinea pig brain nitrophenylphosphatase, at designated Na⁺ concentration. X axis: K⁺ concentration in mM; Y axis: relative nitrophenylphosphatase activity. (A) Aqueous, no ATP. (B) Aqueous, 0.1 mM ATP; (C) 20% Me₂SO, no ATP.

present at 5 mM Na^+ , but 20 mM Na^+ transforms this to a sigmoid curve with higher K^+ affinity. In the absence of ATP, as in Fig. 2a, the enzyme is less sensitive to Na^+ . Fig. 2c shows that, in Me_2SO , the transition occurs at relatively low Na^+ concentration even in the absence of ATP.

Effects of Na^+ , ATP and Me_2SO on K^+ activation

K^+ activation of nitrophenylphosphatase in the presence of several different constant Na^+ concentrations was measured in the presence and absence of 0.1 mM ATP and 20% Me_2SO . The results are shown in Figs 3a–d for beef brain. The results obtained using guinea pig brain enzyme were essentially identical and are not shown. In the absence of ATP and Me_2SO , only a slight decrease in activity with increasing Na^+ is seen until a relatively high Na^+ concentration is present, and then activation is small. In either 0.1 mM ATP or Me_2SO intermediary plateaus and activation appear at a much lower Na^+ concentration, but K^+ affinity without Na^+ is decreased by ATP and increased by Me_2SO . In the presence of both ATP and Me_2SO , activation occurs at a still lower Na^+ concentration.

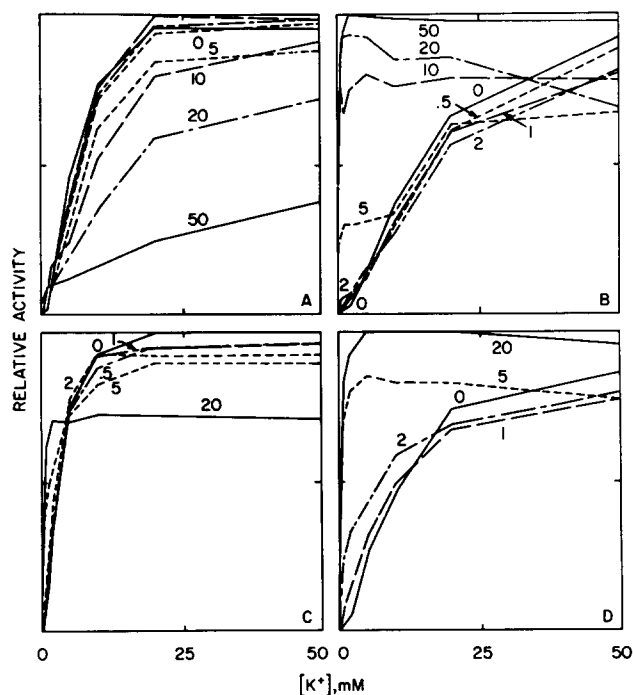


Fig. 3. K^+ activation of beef brain nitrophenylphosphatase, at designated Na^+ concentration. X axis: K^+ concentration in mM; Y axis: nitrophenylphosphatase activity. Relative rates, determined at $[\text{K}^+] = 0.1, 0.2, 0.5, 1, 2, 5, 10, 20$ and 50 mM, are connected by straight lines. The computed V for each set of conditions is shown in Fig. 7. (A) Aqueous, no ATP; (B) Aqueous, 0.1 mM ATP; (C) 20% Me_2SO , no ATP; (D) 20% Me_2SO , 0.1 mM ATP.

Effect of K^+ on nitrophenylphosphatase substrate activation parameters

Nitrophenylphosphatase activity was measured as a function of nitrophenylphosphate concentration at a series of fixed K^+ levels. When the data were fitted to the Hill equation, Hill coefficients for substrate activation ranged from 1.1 to 1.35 and did not vary systematically with increasing K^+ . However, the K values were found to decrease (Fig. 4a) and the V values were found to increase (Fig. 4b) with increasing K^+ .

The dashed lines (Figs 4a and 4b) show the K and V values obtained from computer fitting of nitrophenylphosphate activation of nitrophenylphosphatase in the presence of 100 μ M ATP. K is increased by ATP at all concentrations of K^+ . V is decreased by ATP at any K^+ concentrations but the extrapolated V at infinite K^+ is not affected by ATP.

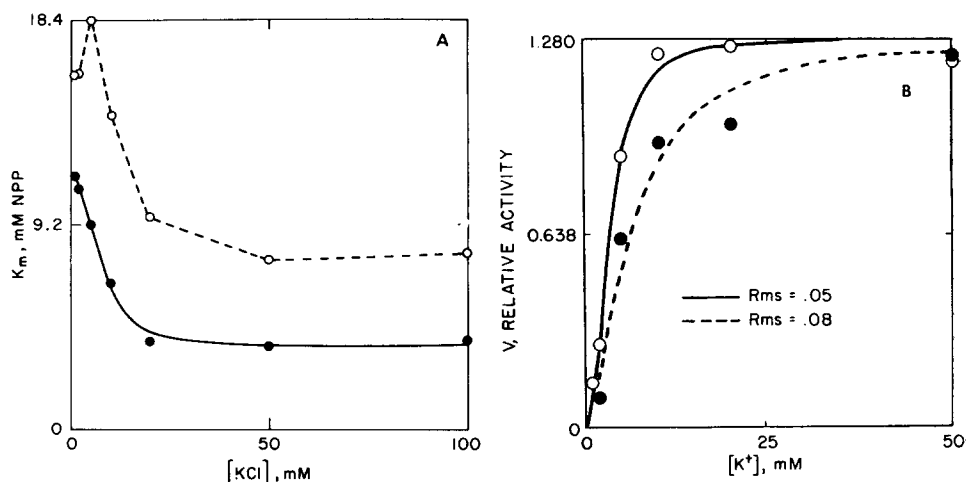


Fig. 4. Effect of KCl on the activation of *p*-nitrophenylphosphatase by *p*-nitrophenylphosphate (NPP). (a) Effect on $[NPP]_{0.5}$ v: \bullet — \bullet , no ATP; \circ — \circ , 100 μ M ATP. (b) Effect on V , fitted to Hill equation: \bullet — \bullet , no ATP; \circ — \circ , 100 μ M ATP.

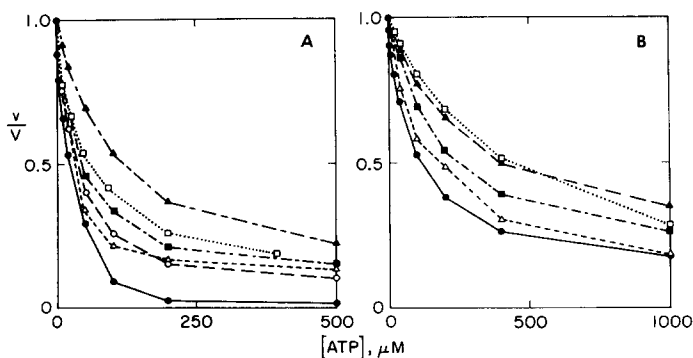


Fig. 5. Inhibition of nitrophenylphosphatase by ATP at various concentrations of K^+ . (a) $[K^+] = 1$ mM, \bullet — \bullet ; 5 mM, \circ — \circ ; 7.5 mM, \triangle — \triangle ; 10 mM, \blacksquare — \blacksquare ; 15 mM, \blacksquare — \blacksquare ; 20 mM, \square — \square ; 25 mM, \blacktriangle — \blacktriangle ; (b) $[K^+] = 25$ mM, \bullet — \bullet ; 30 mM, \circ — \circ ; 50 mM, \triangle — \triangle ; 100 mM, \blacksquare — \blacksquare ; 150 mM, \blacksquare — \blacksquare ; 200 mM, \blacktriangle — \blacktriangle ; 250 mM, \square — \square .

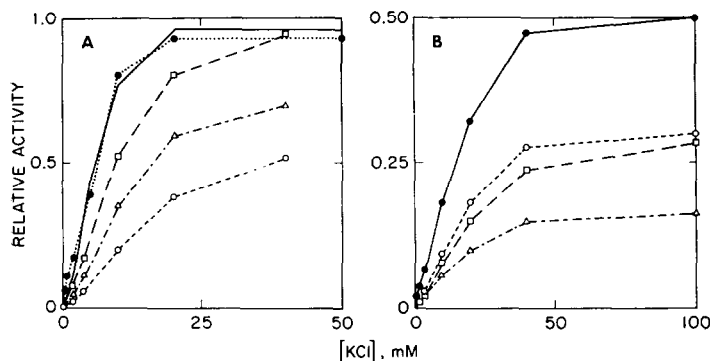


Fig. 6. Activation of nitrophenylphosphatase by K^+ at various ATP concentrations: (a) $[ATP] = 0 \mu M$, —; $10 \mu M$, ●—●; $20 \mu M$, □—□; $50 \mu M$, △—△; $100 \mu M$, ○—○; (b) $[ATP] = 200 \mu M$, ●—●; $500 \mu M$, ○—○; $1000 \mu M$, □—□; $2000 \mu M$, △—△.

ATP inhibition of nitrophenylphosphatase

Nitrophenylphosphatase activity was measured as a function of ATP concentration at a series of different K^+ concentrations (Fig. 5). Activity decreases monotonically with increasing ATP. Increasing K^+ increases the concentration of ATP required for 50% inhibition.

Conversely, when K^+ activation is measured in the presence of different ATP concentrations, increasing ATP increases the concentration of K^+ necessary for 50% of maximal activation and decreases the apparent maximum velocity (Fig. 6).

ATP + Na^+ activation of nitrophenylphosphatase

Nitrophenylphosphatase activity was measured as a function of ATP concentration in the presence of 25 mM NaCl at a series of different K^+ concentrations (Fig. 7). Since preliminary experiments had indicated that the concomitant hydrolysis of ATP under these conditions was sufficient to influence the nitrophenylphosphatase assay, an ATP-regenerating system was employed in these experiments as described under Methods.

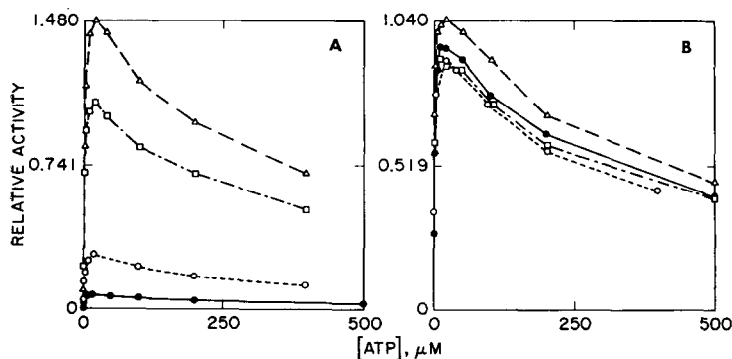


Fig. 7. Activation of nitrophenylphosphatase by ATP in the presence of 25 mM NaCl and various concentrations of K^+ : (a) $[K^+] = 0.5 \text{ mM}$, ●—●; 1 mM , ○—○; 2 mM , △—△; 5 mM , □—□; (b) $[K^+] = 7.5 \text{ mM}$, ○—○; 10 mM , □—□; 15 mM , △—△; 20 mM , ●—●.

At each level of K^+ , a biphasic curve is generated: if $[K^+] < 20$ mM, increasing ATP produces activation above the level obtained with $K^+ + Na^+$ followed by a phase of inhibition which declines monotonically toward zero activity; if $[K^+] > 30$ mM, the initial stimulatory phase is replaced by a high-affinity inhibition (Fig. 8).

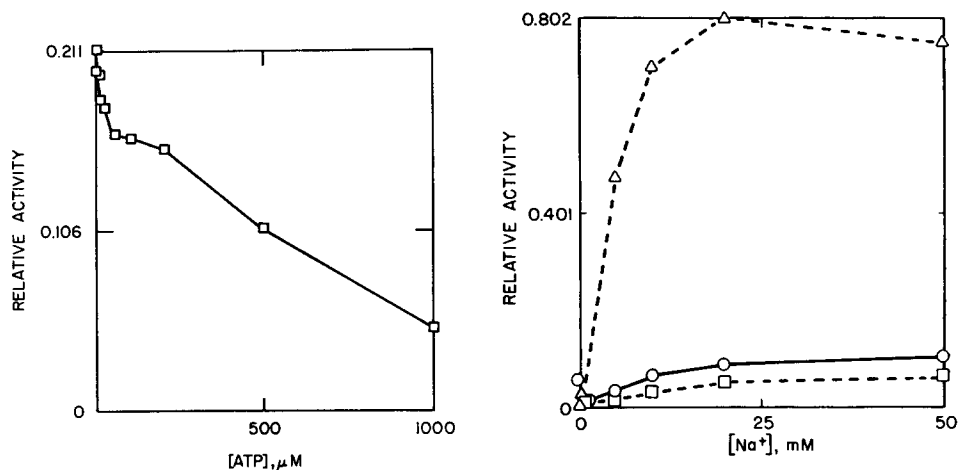


Fig. 8. Inhibition of nitrophenylphosphatase by ATP, in the presence of 25 mM NaCl and 50 mM KCl.

Fig. 9. Activation of nitrophenylphosphate by Na^+ : $[KCl] = 1$ mM; $\bigcirc - \bigcirc$, no nucleotide; $\square - \square$, 100 μ M, β, γ -methylene ATP; $\triangle - \triangle$, 20 μ M ATP.

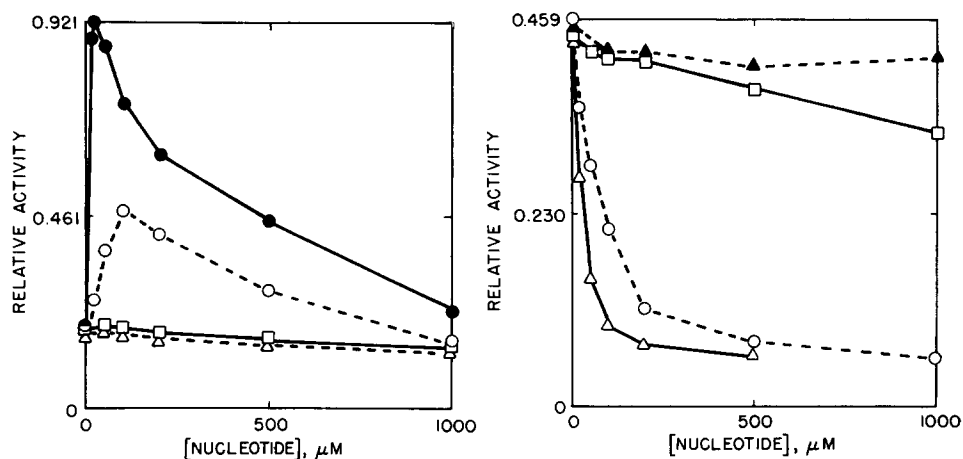


Fig. 10. Activation of nitrophenylphosphatase by various nucleotides: $[KCl] = 5$ mM; $[NaCl] = 25$ mM; $\bullet - \bullet$, ATP; $\bigcirc - \bigcirc$, ADP; $\square - \square$, β, γ -methylene ATP; $\triangle - \triangle$, α, β -methylene ADP.

Fig. 11. Inhibition of nitrophenylphosphatase by various nucleotides: $[KCl] = 5$ mM; nucleotide concentrations as in Fig. 7. $\triangle - \triangle$, ATP; $\bigcirc - \bigcirc$, ADP; $\square - \square$, β, γ -methylene ATP; $\blacktriangle - \blacktriangle$, α, β -methylene ADP.

Effect of analogues of ATP and ADP

Experiments using β,γ -methylene ATP, which does not phosphorylate ATPase [15], and α,β -methylene ADP, which is not a substrate for myokinase as it cannot donate its terminal phosphate, were performed in an attempt to differentiate the effects of phosphorylation from the effects of binding per se.

Fig. 9 shows the effects of β,γ -methylene ATP and ATP on Na^+ activation of nitrophenylphosphatase. Na^+ activation is markedly enhanced by ATP, but β,γ -methylene ATP not only fails to duplicate this effect, but seems to partially inhibit Na^+ activation. In the presence of 25 mM Na^+ , as shown in Fig. 10, neither α,β -methylene ADP nor β,γ -methylene ATP has any effect on nitrophenylphosphatase activity. Stimulation by ADP is less than 1/2 that by ATP and requires ten times more nucleotide; this could arise from ATP produced by myokinase.

Both α,β -methylene ADP and β,γ -methylene ATP cause slight inhibition of nitrophenylphosphatase at relatively low concentrations (Fig. 11). Further inhibition occurs at greater concentrations of β,γ -methylene ATP but not with α,β -methylene ADP.

DISCUSSION

The kinetic data indicate complex interactions among binding sites for each of the ligands considered here. Since even in the simplest cases it is not possible to determine the number of binding sites unambiguously, in this respect the curves must be treated empirically [21]. The simplest function which will generate the appropriate curves is the Hill equation [22] with an additional term to account for competitive effects of the second ligand [11]:

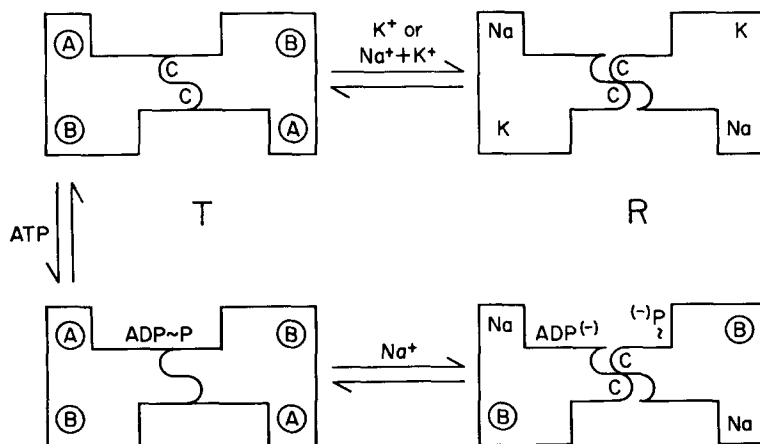


Fig. 12. Dimer relaxation model of ATPase. The "C", or catalytic sites are "exposed" by binding of appropriate cations to the A (sodium) or B (potassium) regulatory sites. ATP is assumed to bind to an adenosine site on one subunit and a phosphoryl acceptor site on the other, stabilizing "T". This is consistent with "half-of-sites" activation; only one molecule of ATP is necessary to drive the $\text{T} \rightarrow \text{R}$ change in a dimer. The dimeric form is shown for simplicity only; any number of subunits is consistent with the model.

$$Y = \frac{(M_1/K_1)^n}{1 + \left(\frac{M_1}{K_1}\right)^n + \left(\frac{M_2}{K_2}\right)^n} \quad (1)$$

This approximation is applied to each of the three sites, Y_a (Na regulatory), Y_b (K regulatory) and Y_c (catalytic). A conservation equation can be written for the regulatory sites:

$$1 = (Y_a + Y'_a)(Y_b + Y'_b) \quad (2)$$

where $Y' = 1 - Y$ or the fraction with empty sites. Assuming that catalytic sites are

TABLE I

CONSTANTS OBTAINED BY FITTING THE DATA OF Figs 4 AND 5 TO Eqn 3

"A" refers to sodium regulatory, "B" to potassium regulatory and catalytic, and "C" to catalytic sites. Constants labeled "1" are activation constants; those labeled "2" describe competitive inhibition by the opposing cation. "N" denotes Hill coefficients. Plus and minus signs refer to the presence or absence of ATP or Me_2SO .

A. Guinea pig brain

0.1 mM ATP	20 % Me_2SO					
	—	+	—	+	—	+
	K_{A1}		$K_{\beta 1}$		K_{C1}	
—	20.7	7.6	7.2	1.8	0.4	0.5
+	7.0	2.3	18.9	6.9	0.1	0.5
	K_{A2}		$K_{\beta 2}$		K_{C2}	
—	300	9	10	1.2	0.3	38.2
+	199	12	3.2	2.2	112	35 000
	N_A		N_β		N_C	
—	5	1.2	2.2	1.7	0.85	1.0
+	4.5	2.8	1.8	1.9	1.0	1.0

B. Beef brain

0.1 mM ATP	20 % Me_2SO					
	—	+	—	+	—	+
	K_{A1}		$K_{\beta 1}$		K_{C1}	
—	26.3	4.6	5.4	2.9	0.04	0.33
+	5.8	2.3	15.9	9.1	0.14	0.26
	K_{A2}		$K_{\beta 2}$		K_{C2}	
—	166	6.3	8.5	3.0	0.33	36
+	15	24	11.8	2.0	58	43
	N_A		N_β		N_C	
—	1.6	1.1	2.0	1.8	1.0	1.6
+	4.2	2.6	1.6	1.7	1.6	1.7

accessible in forms which have one or both regulatory sites occupied by the appropriate cation, the fraction of enzyme with accessible catalytic sites is $1 - Y'_a Y'_b$ and the relative velocity is thus

$$v/V = Y_c(1 - Y'_a Y'_b) = Y_c(Y_a + Y_b - Y_a Y_b) \quad (3)$$

Curves generated by this equation can closely simulate the experimental observations for the *Electrophorus enzyme* [11]. For purpose of curve fitting a reduction in the number of parameters can be made by the further approximation that $Y_b Y_c = Y_\beta$. Under conditions of zero Na^+ , the parameters V , $K_{\beta 1}$ and N_β can be obtained by fitting to a simple Hill equation. The remaining seven parameters can be obtained by least squares fitting of experimental data to the equation

$$v = V[Y_a Y_c + (1 - Y_a)Y_\beta] \quad (4)$$

Attempts to simulate these data by equations with fewer parameters were unsuccessful [11]. Recently, Skou [23] presented data demonstrating the intermediary plateau phenomenon in beef brain nitrophenylphosphatase. We were not able to simulate this phenomenon in terms of the two-site model which he proposed [11].

Fitting of the data obtained from guinea pig and beef brain under the conditions studied yielded satisfactory approximations with low root means squared error

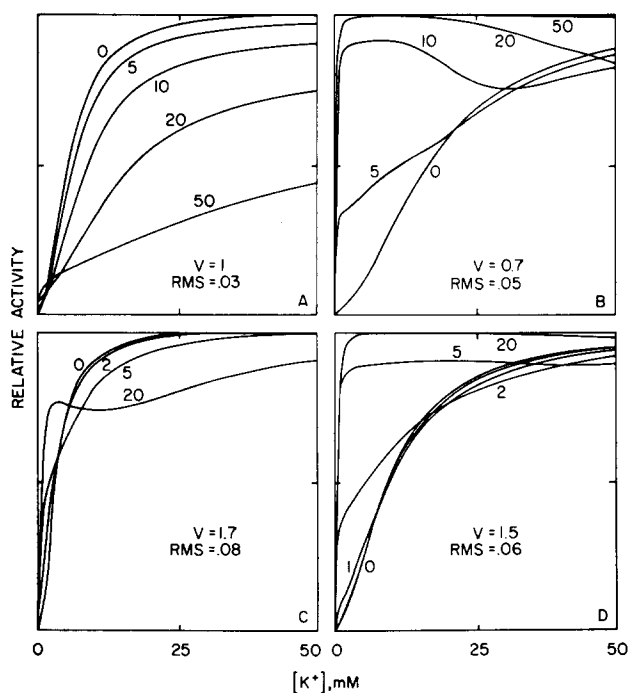


Fig. 13. Fit of data in Fig. 5 to Eqn 4, simulating K^+ activation of beef brain nitrophenylphosphatase at various Na^+ concentrations. In cases of low Na^+ concentrations where curves were not significantly different from that of no Na^+ , the curves are not shown. (A) Aqueous; no ATP. (B) Aqueous, 0.1 mM ATP. (C) 20 % Me_2SO , no ATP. (D) 20 % Me_2SO , 0.1 mM ATP.

and dependency values. The parameters of activation are given in Table I. The experimental data were fitted to Eqn 4 with the MLAB procedure, showing good qualitative agreement in both guinea pig and beef brains; the curves generated by the fit to beef brain are shown in Fig. 13a–d, and can be compared to the actual data in Fig. 3a–d. The simulations of guinea pig data were quite similar.

Several trends involving Me_2SO and ATP effects are evident. The major parallel effects of Me_2SO and ATP occur at sites involving Na^+ . Most obvious are the decreases in K_{A1} , leading to conversion of enzyme to the active form at lower Na^+ concentration. These effects, furthermore, are additive. While increasing Na^+ affinity for activation at the “A” site, however, Me_2SO and ATP decrease Na^+ affinity for inhibition at the “C” or catalytic site: in the absence of Me_2SO or ATP, inhibition of this site is marked even at low Na^+ concentration; in their presence, there is essentially no sodium inhibition. Thus, ATP and Me_2SO exhibit synergism with Na^+ both by enhancing activation and by decreasing inhibition by sodium on different sites.

ATP and Me_2SO also act in parallel on potassium inhibition of the “A”, or Na^+ , site. Their action here is opposite to that on the “C” site, but numerically less important.

While acting similarly on Na^+ sites, the major effects of ATP and Me_2SO oppose each other at K^+ sites. Me_2SO raises the affinity for K^+ at the “B” site, while ATP diminishes K^+ affinity; the effect of ATP+20% Me_2SO is intermediate between the effects of ATP or Me_2SO alone. Me_2SO , in general, increased the affinity of both Na^+ and K^+ regulatory sites for either ion, decreasing K_{A1} , $K_{\beta1}$, K_{A2} , and $K_{\beta2}$ in both guinea pig and in beef. However, it decreased both cation affinities of the “C” or catalytic site though this effect is not consistently impressive. The relation of these effects to the action of Me_2SO on hydrophobic interactions in this lipid-dependent membrane enzyme remains to be determined. The Me_2SO effects on mammalian enzyme are less than on the eel enzyme, whereas ATP effects are very small in the case of eel enzyme. ATP and Me_2SO evidently exert their effects through quite different mechanisms which nonetheless converge at several points.

ATP increased N_A , from 1.6 to 4.2 in beef without Me_2SO , and from 1.1 to 2.6 in the presence of 20% Me_2SO . While N_A is > 5 in guinea pig brain without ATP, this value could be varied widely without effecting other parameter values (this was not the case for constants elsewhere). ATP also increases n for nitrophenylphosphate activation of nitrophenylphosphatase. A Hill coefficient of 4 could signify the presence of 4 interacting subunits, though the involvement of Na^+ and K^+ sites in coupled transport and the complexity of the binding site interactions prevent interpretation [11]. It should be emphasized that sigmoidicity in the activation curves is not a necessary component of the heterotropic relaxation model; if all of the Hill coefficients are set equal to unity, this model would still qualitatively describe the data, including the intermediary plateaus, but the ability to quantitatively fit the data would be considerably impaired.

Intermediary plateaus and maxima such as those which Na^+ induces into the K^+ -activation curves of nitrophenylphosphatase have been described for a number of substrate vs activation curves [12]. This phenomenon can be incorporated into model equations by introducing heterogeneity into some of the subunit parameters of oligomeric models or by postulating a mixture of isozymes with differing ligand affinities [12]. In the nitrophenylphosphatase, the existence of intermediary plateaus

or maxima is dependent upon the presence of Na^+ and sigmoid activation occurs again at higher levels of Na^+ . At the present stage of uncertainty about the subunit composition of $(\text{Na}^+ + \text{K}^+)\text{-ATPase}$, a model which attributes intrinsic binding constants to specific subunits has little factual basis.

The present heterotropic relaxation model is formally similar to the "two parallel pathways" proposal of Robinson [14, 24], since one might regard access of the substrate to the catalytic site via occupation of sites B and C by K^+ as a pathway distinct from that permitted by $\text{Na}^+ + \text{K}^+$ occupation of sites A and C. Robinson's equation permits the two pathways to have different V values. His data, as well as our own, can be adequately fit by a single V , in which case the two equations become identical.

The properties of Na^+ - and K^+ -binding sites have been investigated by measuring their effects on the rate of ouabain binding [14]. Lindenmayer et al. [25] have described a site which binds K^+ ($K_D = 0.2 \text{ mM}$) and Na^+ here. Effects at this site could be described by simple competitive binding of Na^+ and K^+ only if the measurements were made in the presence of $>10 \text{ mM Na}^+$. As ATP is present in these experiments, this would correspond to near saturation of the A site in our model. Effects of the B site would become evident in these experiments only through effects of K^+ measured in the absence of Na^+ .

Interactions of ATP with nitrophenylphosphatase and K^+

In the presence of less than 2 mM K^+ , ATP inhibition is essentially non-competitive with respect to nitrophenylphosphate. As K^+ is increased, the competitive component of ATP inhibition increases, and predominates with K^+ in excess of 4 mM (Fig. 14).

The apparent affinity of ATP as an inhibitor of nitrophenylphosphatase (Fig. 5) is a sigmoid function of K^+ concentration (Fig. 15). ATP is a better inhibitor at low K^+ than at high. In terms of the relaxation model, we propose that ATP binds to the T enzyme with high affinity and inhibits nitrophenylphosphate hydrolysis

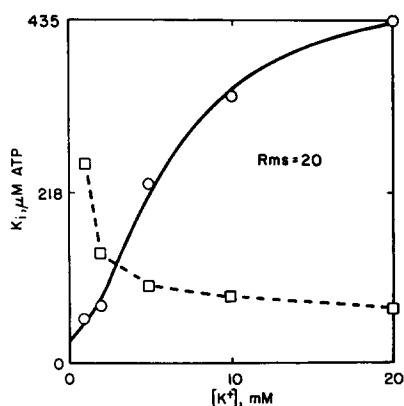


Fig. 14. K_i for nitrophenylphosphatase inhibition by ATP. The data of Fig. 3 were fitted to the Hill equation, and values for K_i obtained from: Competitive $K_i = [\text{ATP}]/(K_{\text{obs}}/K_0 - 1)$; non-competitive $K_i = [\text{ATP}]/(V_0/V_{\text{obs}} - 1)$ where K_0 and V_0 represent K and V in the absence of ATP. $\circ - \circ$, non-competitive K_i ; $\square - \square$, competitive K_i .

allosterically. If this were the only mode of ATP inhibition, it should be entirely competitive with K^+ binding at its "B" or regulatory site. However, the ATP inhibition which is non-competitive with K^+ is proposed to reflect the competitive component of ATP interaction with nitrophenylphosphate. This would be a steric competition at the catalytic site of the R enzyme as discussed above. These concepts can be expressed by equations which permit one to estimate the apparent dissociation constants for ATP binding to the T and R enzymes respectively.

The values of $[ATP]_{0.5v}$ (Fig. 15) were obtained by fitting the data of Fig. 5 to the equation.

$$\frac{v}{V} = \left(\frac{[ATP]^n}{[ATP]_{0.5v}^n} + 1 \right)^{-1} \quad (5)$$

It is evident that $[ATP]_{0.5v}$ will have lower and upper boundary values, K_T and K'_R , as K^+ varies from zero to infinity. Accordingly, $[ATP]_{0.5v}$ is a function of K^+ occupation of the "B" regulatory site:

$$[ATP]_{0.5v} = \frac{K_B^n \cdot K_T + [K^+]^n \cdot K'_R}{K_B^n + [K^+]^n} \quad (6)$$

The results of fitting the data of Fig. 15 to this equation give the following values: $K_B = 32 \text{ mM } K^+$; $n = 1.96$; $K_T = 15 \mu\text{M ATP}$; $K'_R = 246 \mu\text{M ATP}$. Since K'_R represents ATP dissociation from a nitrophenylphosphate binding site measured in the presence of 10 mM nitrophenylphosphate, estimation of the "true" K_R requires correction for this competitive displacement using the expression

$$K_R = \frac{[\text{nitrophenylphosphate}]_{0.5v}}{[\text{nitrophenylphosphate}]_{0.5v} + [\text{nitrophenylphosphate}]} \cdot K'_R \quad (7)$$

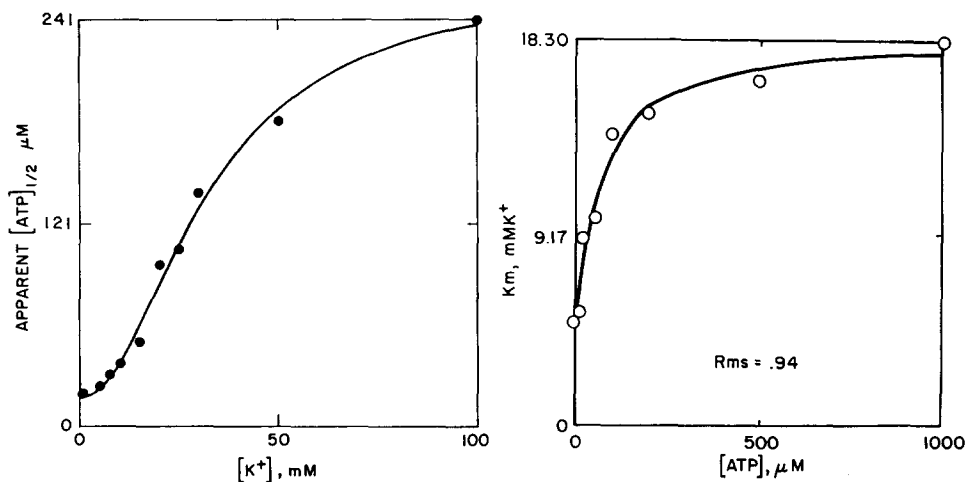


Fig. 15. Concentration of ATP required for half-inhibition of nitrophenylphosphatase, fitted to Eqn 5 (see text).

Fig. 16. K^+ required for half-maximal activation of nitrophenylphosphatase ($K_{\beta 1}$) as a function of ATP; fitted to the Hill equation, maximum $K_{\beta 1} = 18.5 \text{ mM KCl}$; $[ATP]_{0.5} = 67.8 \mu\text{M ATP}$.

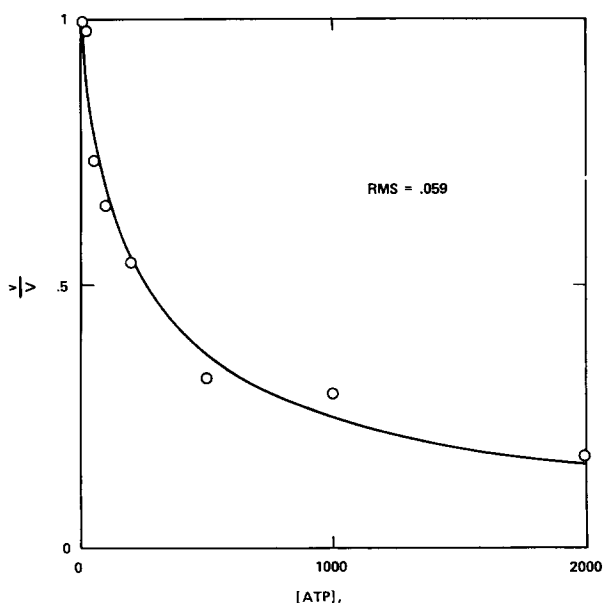


Fig. 17. Maximum K^+ activation of nitrophenylphosphatase as a function of $[ATP]$; extrapolated V at infinite ATP is 0; apparent $[ATP]_{0.5} = 247 \mu M$, corrected $[ATP]_{0.5} = 71 \mu M$ (see text).

which yields a K_R value of $70 \mu M$ ATP.

The data describing K^+ activation of nitrophenylphosphatase at different constant levels of ATP (Fig. 6) were fitted to the Hill equation. As ATP concentration increases, $[K^+]_{0.5}$ increases and V_{K^+} decreases. Competitive and non-competitive components of the ATP- K^+ interaction are concurrent. These data are essentially similar to those summarized in Fig. 15. However, these are derived from separate experiments, extend to higher levels of ATP and to more closely spaced levels of low K^+ . The activation curves derived in this way permit a more conventional separation of competitive (Fig. 16) and non-competitive (Fig. 17) components of ATP inhibition. By the assumptions discussed above, K_R can be derived from Fig. 17 and is identical with that derived from Fig. 15. However, the competitive $[ATP]_{0.5}$ ($68 \mu M$) which can be extracted from Fig. 16 represents ATP inhibition when the B site is half saturated with K^+ , and thus is a mixed constant resulting from binding to both T and R enzymes.

Effect of Na^+ on ATP- K^+ interactions

The synergism of ATP with ($Na^+ + K^+$) activation of nitrophenylphosphatase has been mentioned above and is reflected in the lowering of K_{A1} by ATP. Low concentrations of ATP produce this synergism primarily by (1) increasing the apparent affinity of Na^+ for the Na^+ -regulatory site and (2) by increasing the selectivity of the catalytic site for K^+ relative to Na^+ . The data of Figs 9 and 10 are consistent with the hypothesis that phosphorylation is involved in ATP- Na^+ synergism. We have examined K^+ activation as a function of ATP concentration in the presence of saturating levels of Na^+ (Fig. 7). A family of biphasic curves is obtained by varying the level of ATP at different fixed concentrations of K^+ . These curves can be simulated by an

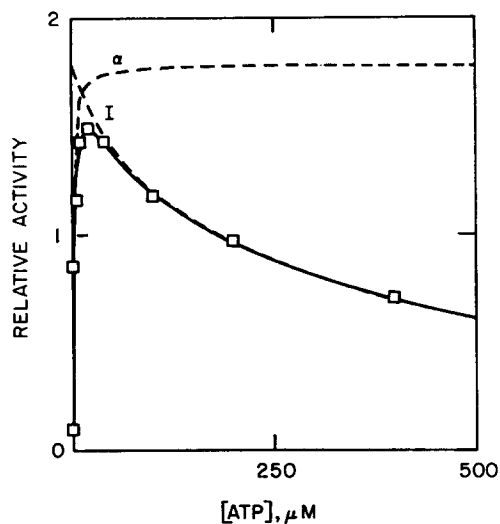


Fig. 18. Activation of nitrophenylphosphatase by ATP, 25 mM NaCl and 1 mM KCl. The data, taken from Fig. 4, are fitted to Eqn 4 (solid line). The dashed lines represent the activation (a) and inhibition (I) phases of Eqn 4.

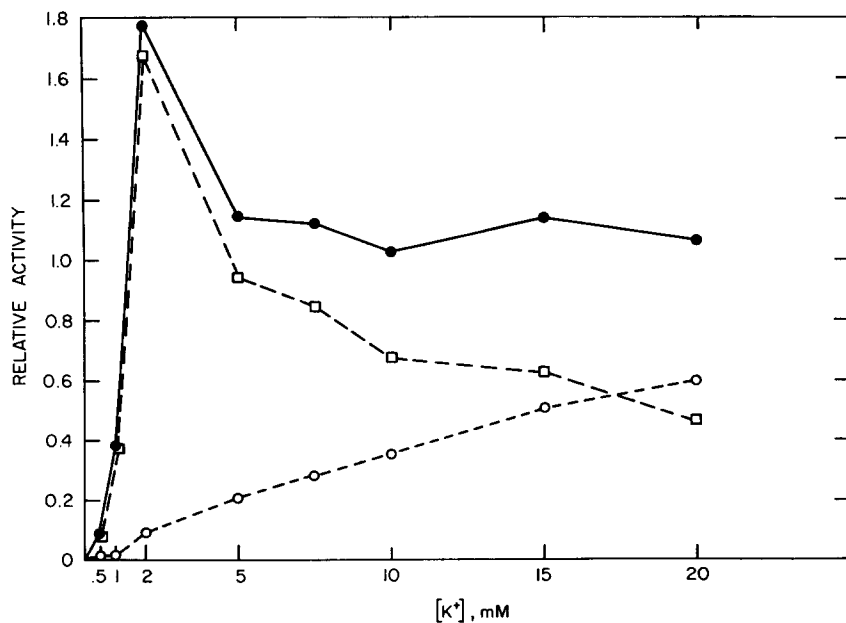


Fig. 19. Components of ATP activation of nitrophenylphosphatase at various concentrations of KCl (see Eqn 4): \bullet — \bullet , calculated maximum total velocity; \square — \square , calculated maximum activation by ATP (V_a); \circ — \circ , velocity in the absence of ATP (V_0).

equation which includes an activating constant for the combination of ATP with T enzyme and a term for non-competitive inhibition of the R enzyme (Fig. 18)

$$v = \left(V_0 + \frac{V_a [\text{ATP}]^m}{K_a^m + [\text{ATP}]^m} \right) \left(\frac{K_i^n}{K_i^n + [\text{ATP}]^n} \right) \quad (8)$$

The constant V_0 is established from K^+ activation in the absence of ATP; V_a , K_a , K_i , m and n have been obtained by computer fitting. Systematic changes occurred in V_a (Fig. 19), but not in the other constants. The apparent inhibition constant for ATP in the presence of Na^+ , K_i , is $257 \mu\text{M}$. This should also be corrected according to Eqn 3 and is essentially identical with the values obtained for inhibition of the R enzyme in the absence of Na^+ . Thus ATP inhibition of K^+ -activated phosphatase may be attributed to the same site which produces ATP inhibition of the $(\text{Na}^+ + K^+)$ -activated phosphatase.

In the presence of Na^+ the apparent binding constant for ATP activation, K_a , is only $2.6 \mu\text{M}$. This apparently high affinity may have a different explanation. The ATPase mechanism can be written in the following abbreviated form as a series of essentially irreversible steps:



If we assume that E_R is the only form which hydrolyses nitrophenylphosphate, then

$$\frac{v}{V} = \frac{\text{E}_\text{R}}{\text{E}_{(\text{total})}} = \left(\frac{k_3}{k_1 [\text{ATP}]} + \frac{k_3}{k_2} + 1 \right)^{-1} \quad (10)$$

and increasing concentrations of ATP will produce the observed activation of nitrophenylphosphate hydrolysis in the presence of Na^+ and K^+ . If $k_2 \gg k_3$, the $[\text{ATP}]_{0.5 v}$ for activation would approximate k_3/k_1 .

Thus the apparent affinity of ATP in the presence of Na^+ may actually be the ratio of two forward rate constants. By this hypothesis, the phosphorylated enzyme is not itself able to hydrolyse nitrophenylphosphate, but hydrolysis of $\text{E}-\text{P}$ brings the enzyme into the active state. Since Na^+ and K^+ each can activate nitrophenylphosphatase in the absence of ATP, this is only one of at least 3 parallel pathways which influence the distribution of enzyme conformers.

Model for the ATP interactions

These and previous studies delineate three types of nucleotide interaction with *p*-nitrophenylphosphatase: (i) inhibition which is competitive with K^+ and non-competitive with *p*-nitrophenylphosphate; (ii) inhibition which is non-competitive with K^+ and competitive with *p*-nitrophenylphosphate; (iii) activation by ATP in the presence of Na^+ . All three interactions can be reconciled with a single nucleotide-binding site through an extension of the relaxation model previously proposed [11, 13]. The discussion arbitrarily assumes a dimer of identical subunits. The nucleotide effects can be explained through this model as follows: (i) the T conformation is

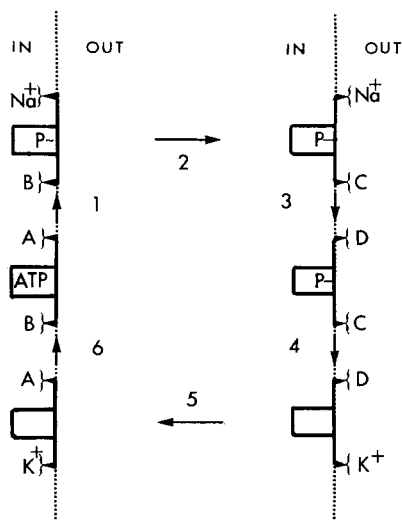


Fig. 20. Illustration of coupling of low and high affinity forms of Na^+ and K^+ ionophoric sites. The Na^+ site has a high-affinity intracellular form (A) and a low-affinity extracellular form (D). The K^+ site has a low-affinity intracellular form (B) and a high-affinity extracellular form (C) (see text).

inactive as a *p*-nitrophenylphosphatase and is stabilized with respect to the R conformation by nucleotide binding; the R conformation is active as a *p*-nitrophenylphosphatase and is stabilized with respect to the T conformation by K^+ binding at B sites; thus K^+ and nucleotide binding are competitive; (ii) at saturating concentrations of both ligands, the K^+ effect prevails; however, under these conditions ATP can compete with *p*-nitrophenylphosphate at the phosphate catalytic site; (iii) the T conformation, in the presence of Na^+ , is a protein phosphokinase; ATP bound to the T conformation in the presence of Na^+ phosphorylates the enzyme; the phosphorylenzyme is most stable in the R conformation; the phosphorylenzyme is not an active *p*-nitrophenylphosphatase, but in the presence of K^+ it is rapidly hydrolysed to the active form.

In Fig. 12 a single nucleotide-binding site is depicted as an area encompassing portions of two opposed subunits. Nucleotides could stabilize the T conformation by crosslinking the subunits at this site. The mechanism need not be so direct as this. However, the crosslinking concept is convenient in that it also provides a possible explanation of the $\text{Na}^+ + \text{ATP}$ activation: if the adenyl-binding locus and the phosphoryl-acceptor locus are on different subunits, the electrostatic repulsion between enzyme acylphosphate and enzyme-bound ADP could promote the transition from T to R conformation.

Coupling of ATP hydrolysis to cation transport

The first evidence which led to proposals for conformational transitions linked to ATP hydrolysis were derived from studies of the phosphoryl enzyme and of the Na^+ -dependent ATP/ADP transphosphorylation [2, 26]. These experiments did not provide information about different classes of cation-binding sites. Since Na^+ and K^+ act principally at separate stages of the reaction sequence, it has commonly been

assumed that they could be transported alternately by a single type of ionophoric site which has conformationally dependent orientation and selectivity [1].

The more recent evidence indicates a greater complexity. In particular, separate sites for Na^+ and K^+ exist. Although these sites have not been shown to be ionophores, a reasonable hypothesis can be advanced on the assumption that they are. Fig. 20 indicates how all of the ligand sites which have been defined by these studies can be assigned functional roles in active transport. The A and B sites of the relaxation model are equated with the cytoplasmically oriented ionophores for Na^+ and K^+ respectively. The extracellular configurations of these same ionophores are denoted D and C respectively. The D site is a previously unidentified low-affinity Na^+ site which, although not apparent in the nitrophenylphosphatase kinetics, is required for the symmetry of this scheme. Taniguchi and Post [27] have obtained evidence for the required low-affinity Na^+ site in their studies of ATP synthesis by reversal of the conformational cycle.

An essential feature of this concept is that the Na^+ and the K^+ ionophores are coupled together with regard to their orientation in the membrane. Cation selectivity is linked to orientation so that A and C are the relatively high-affinity forms of the Na^+ and K^+ ionophores. For active transport to occur, the low-affinity forms must generally traverse the membrane in "free" form. The affinity of the A site for Na^+ may be increased by ATP binding as concluded by Skou [23] and the affinity of the B site for K^+ may be reduced by ATP binding as indicated by several studies [28–30]. However, these effects of ATP may be mediated entirely through alterations in the equilibria between conformers.

Implications of the model for the stoichiometry of active transport

The steady-state kinetic description of the *p*-nitrophenylphosphatase has led to three major conclusions: (a) three distinct classes of univalent cation-binding sites are required to account for the kinetic effects of Na^+ and K^+ ; (b) a single nucleotide-binding site is sufficient to account for the kinetic effects of nucleotides; (c) both the univalent cation kinetics and the nucleotide kinetics are consistent with an enzyme which can exist in two states with respect to the activity of the catalytic site.

In principle these conclusions do not require an oligomeric enzyme, much less an oligomeric enzyme of identical subunits. Interactions between identical subunits remains attractive because it can explain the physiological data which indicate that several cations are transported for each molecule of ATP hydrolysed. In the case of erythrocytes [8, 9], the data indicate a rather fixed stoichiometry of $\text{ATP} : \text{Na}^+ : \text{K}^+$. In squid giant axons, the cation gradients and the metabolic state seem to determine the stoichiometries [10].

Efficient operation of active transport over a range of micro-environments would seem to require a variable stoichiometry. The model discussed here provides a mechanism which would produce variable ratios between moles of ATP hydrolysed and equivalents of cations transported. This can be outlined as follows: vectorial transport forces arise from the conformational transitions which in turn are driven by the phosphorylation cycle. There is conformational coupling among identical subunits which is postulated to be in phase. Phosphorylation of a single subunit might be sufficient to induce conformational transitions, and hence vectorial transport, in two or more coupled subunits. Each subunit need have only a single ionophoric site

for each cation. Conditions which are energetically less favorable for the conformational transition (e.g. high opposing cation gradients) would increase the probability of multiple phosphorylations of an oligomeric enzyme within the kinase phase of the cycle. This mechanism would imply the type of negative cooperativity with respect to ATP that has been observed [31] and could lead to half-of-sites reactivity with respect to enzyme phosphorylation as has also been reported [32].

The implications of negative cooperativity among clusters of membrane-bound subunits are discussed by Levitski with respect to the "spare receptor" theory of drug-receptor interaction [33]. Many of his conclusions are applicable to the problem of variable stoichiometry in active transport.

REFERENCES

- 1 Albers, R. W., Koval, G. J. and Siegel, G. J. (1968) *Mol. Pharmacol.* 4, 324-336
- 2 Post, R. L., Kume, S., Tobin, T., Orcutt, T. and Sen, A. K. (1969) *J. Gen. Physiol.* 54, 306s-326s
- 3 Robinson, J. D. (1967) *Biochemistry* 6, 3250-3258
- 4 Repke, K. R. H. and Schoen, R. (1973) *Acta Biol. Med. Germ.* 31, K19-30
- 5 Stein, W. D., Lieb, W. R., Karlsh, S. J. D. and Eilam, Y. (1973) *Proc. Natl. Acad. Sci. U.S.* 70, 275-278
- 6 Robinson, J. D. (1974) *Biochim. Biophys. Acta* 341, 232-247
- 7 Lazdunski, M. (1972) *Curr. Top. Cell. Regul.* 6, 267-310
- 8 Sen, A. K. and Post, R. L. (1964) *J. Biol. Chem.* 239, 345-352
- 9 Whittam, R. and Ager, M. E. (1965) *Biochem. J.* 97, 214-227
- 10 Mullins, L. J. (1972) *Role of Membranes in Secretory Processes*, pp. 182-202, North-Holland, Amsterdam
- 11 Albers, R. W. and Koval, G. J. (1973) *J. Biol. Chem.* 248, 777-784
- 12 Tiepel, J. and Koshland, D. E. (1969) *Biochemistry* 8, 4656-4663
- 13 Albers, R. W., Koval, G. J. and Swann, A. C. *Ann. N.Y. Acad. Sci.*, in the press
- 14 Robinson, J. D. (1970) *Arch. Biochem. Biophys.* 139, 164-171
- 15 Yoshida, H., Nagai, K., Ohashi, T. and Nakagawa, Y. (1969) *Biochim. Biophys. Acta* 171, 178-185
- 16 Albers, R. W. and Koval, G. J. (1972) *J. Biol. Chem.* 247, 3088-3092
- 17 Nakao, T., Tashima, Y., Nagano, K. and Nakao, M. (1965) *Biochem. Biophys. Res. Commun.* 19, 755-758
- 18 Knott, G. D. and Reece, D. K. (1972) *Proc. Online Conf.* 1, 497
- 19 Mayer, M. and Avi-Dor, Y. (1969) *Isr. J. Chem.* 7, 139
- 20 Mayer, M. and Avi-Dor, Y. (1970) *Biochem. J.* 116, 49-54
- 21 Frieden, C. (1967) *J. Biol. Chem.* 242, 4045-4052
- 22 Hill, A. V. (1910) *J. Physiol. (London)* 40, IV-VIII
- 23 Skou, J. C. (1974) *Biochim. Biophys. Acta* 339, 246-257
- 24 Robinson, J. D. *Ann. N.Y. Acad. Sci.*, in the press
- 25 Lindenmayer, G. E. and Schwartz, A. (1973) *J. Biol. Chem.* 248, 2191-2300
- 26 Fahn, S., Koval, G. J. and Albers, R. W. (1966) *J. Biol. Chem.* 241, 1882-1880
- 27 Taniguchi, K. and Post, R. L. (1974) *Fed. Proc.* 33, 1289
- 28 Hegyvary, C. and Post, R. L. (1971) *J. Biol. Chem.* 246, 5234-5240
- 29 Norby, J. G. and Jensen, J. (1971) *Biochim. Biophys. Acta* 233, 104-116
- 30 Siegel, G. J. and Goodwin, B. (1972) *J. Biol. Chem.* 247, 3630-3637
- 31 Neufeld, A. H. and Levy, H. M. (1969) *J. Biol. Chem.* 244, 6493-6497
- 32 Norby, J. G. and Jensen, J. *Ann. N.Y. Acad. Sci.*, in the press
- 33 Levitski, A. (1974) *J. Theor. Biol.* 44, 367-372